Recalculating Total Number of e-folds in Loop Quantum Cosmology in View of Generalized Reheating

Yogesh*
Institute for Theoretical Physics and Cosmology, Zhejiang University of Technology, Hangzhou, 310032, China

Mayukh R. Gangopadhyay†
Centre for Cosmology and Science Popularization, SGT University, Gurugram, Haryana-122505, India

Anzhong Wang‡
GCAP-CASPER, Physics Department, Baylor University, Waco, TX 76798-7316, USA

In loop quantum cosmology, the slow-roll inflation is generic, and when the kinetic energy of the scalar field dominates at the bounce, the evolution of the Friedmann–Lemaître–Robertson–Walker universe will go through three distinguishable epochs, bouncing, transition, and finally slow-roll inflation, before the reheating commences. The bouncing dynamics are insensitive of the potential and initial conditions, so that the expansion factor and the scalar field can be described uniquely by a universal solution during this epoch. After about 10^5 Planck time, the epoch of transition starts and the universe rapidly turns over from the kinetic energy dominated state to the potential energy dominated one, whereby the slow-roll inflationary phase begins. In this paper, we consider the power law plateau potential and study the pre-inflationary cosmology for different sets of initial conditions, so that during the slow-roll inflation epoch enough e-folds will be produced. Considering the generalized reheating and comparing with the recent Planck 2018 data we are able to constrain the total number of e-folds (N_T) from the bounce till today to be consistent with the current observable universe. Depending on the matter driving the reheating (subject to the different dominant equations of states), we report the observationally allowed N_T and reheating temperature and find in particular $N_T \simeq 127$, which is significantly different from the one $N_T \gtrsim 141$ obtained previously without considering the reheating phase.

I. INTRODUCTION

The inflationary scenario is a unique and convincing paradigm that serves as one of the cornerstones of contemporary cosmology. A brief phase of rapid expansion that occurred at the initial instant of the universe, just before the radiation-dominated epoch is referred to as cosmological inflation. At first, inflation was used to solve the shortcomings of the Big Bang models, including the horizon and flatness problems [1–6]. A successful inflationary model should predict a quasi-adiabatic and almost Gaussian primordial spectrum of perturbations, with spectral properties consistent with the Cosmic Microwave Background (CMB) observations [7–10]. However, despite the fact that inflation is an elegant paradigm and solve various problems of the big bang universe, it fails to address other fundamental issues of the early universe, such as the origin and nature of the fields, which drive the inflation known as inflaton fields, Big Bang singularity and dynamics before the preinflationary phase. In particular, the success of the inflationary scenario depends heavily on our ability to comprehend the ultraviolet (UV) physics. For the inflationary models which require the number of e-folds more than 70 it becomes doubtful whether the underlying quantum field theory on a classical spacetime is reliable or not [11]. This is because these theories treat spacetime as classical when the size of the current universe is smaller than the Planck size at the beginning of inflation and this gives rise to the trans-Planckian problem [12, 13]. Furthermore, the initial singularity is still inevitable [14, 15]. On the other hand, loop quantum cosmology (LQC) presents a compelling explanation for preinflationary physics which can resolve these issues. In LQC the singularity at Big Bang is replaced by a quantum bounce where the universe transitions from a contracting phase to an expanding phase without hitting the singularity [16–18]. LQC now becomes a well-established branch of Loop Quantum Gravity (LQG), a quantum gravity theory created to solve the issues of combining quantum mechanics with general relativity, and has the potential to act as a quantum gravity extension for a range of cosmological models, including inflation, ekpyrotic, and matter bounces [18–58]. In the conventional

* yogeshjjmi@gmail.com
† mayukh_ccsp@sgtuniversity.org, mayukhraj@gmail.com
‡ Anzhong_Wang@baylor.edu

inflationary paradigm, the evolutionary trajectory usually initiates well after the Planck era, marked by curvature and energy density of matter fields in the universe approximately a several orders of magnitude lower than the Planck scale, thereby making quantum gravity effects negligible. It is unclear how these pre-inflationary dynamics will be once quantum gravity effects become important. The lack of knowledge regarding earlier cosmic stages is embedded in the selection of initial conditions at the onset of inflation, encompassing both the background homogeneous geometry and cosmological perturbations. The latter is commonly assumed to adhere to the Bunch-Davies vacuum state at the onset of inflation. This assumption is crucial, albeit robust. There is considerable interest in extending this scenario backward in time to encompass the Planck era and demonstrating that these initial conditions (or something akin to them) can arise from the pre-inflationary dynamics when quantum gravity effects become significant. Additionally, in standard inflationary models, the background spacetime exhibits classical singularity, an issue addressed in LQC where quantum gravity effects substitute the big-bang singularity with a non-singular bounce. Similarly, both the ekpyrotic and matter bounce scenarios necessitate a cosmic bounce, a requirement for which LQC offers a natural mechanism. LQC serves as a quantum gravity culmination for these cosmological scenarios, emphasizing the additional aspects introduced into observable quantities through this extension. The novel effects arising from quantum gravity act as a gateway to the cosmic Planck era, offering an opportunity to test the concepts outlined here by comparing predictions with observations of CMB. Thus, LQC provides a complete description of the spacetime geometry of the Planck era for the Friedman-Lemaitre-Robertson-Walker (FLRW) spacetime. An important question to be addressed is whether the quantum bounce and associated pre-inflationary physics can leave some interesting imprints on the current or future cosmological experiments [59, 60]. There are primarily several distinct methods for studying pre-inflationary dynamics and cosmological perturbations [52]. All of these approaches lead to the same set of dynamical equations for the evolution of the background. Therefore, the results we present in this article will be valid in all these approaches. To address the issues of pre-inflationary physics various inflationary models have been considered in the framework of LQC [16, 18], and it was shown explicitly that the slow-roll inflation is generic [61, 62] [1]. In this work, we shall conduct a thorough analysis of the impact of the quantum bounce and the pre-inflationary dynamics on the background evolution. One of the main objectives of this work is to study the effect of generalized reheating on the total number of e-foldings.

The paper is organized as follows: In section II, we have given a short description of the background evolution in the LQC scenario. Here we have chosen a well-motivated Power Law Plateau (PLP) potential for the study. Both analytical and numerical evolution has been studied. In section III, the analysis is carried out for the PLP model. The main finding of this manuscript is given in section IV and the effect of generalized reheating on the total number of e-foldings that our Universe has gone through is reported in section V. Finally, we conclude with our findings and future directions in this context of LQC in the last section VI.

II. BACKGROUND EVOLUTION

The modified Friedmann equation in the LQC can be written as [65–67] (see also [41] for an alternative approach):

$$H^2 = \frac{8\pi}{3m_{\rm Pl}^2}\rho\left(1-\frac{\rho}{\rho_{\rm c}}\right), \tag{2.1}$$

where $H \equiv \dot{a}/a$ represents the Hubble parameter and the dot stands for the derivative concerning the cosmic time t, also we use $m_{\rm Pl} = 1/\sqrt{G}$ is the Planck mass. Here ρ and $\rho_{\rm c}$ denote the energy density and critical energy density respectively, and the maximum value of the critical energy density can be attained in the LQC is about $\rho_{\rm c} \simeq 0.41 m_{\rm Pl}^4$. The occurrence of a non-singular quantum bounce, which eliminated the initial singularity in the early stages of the classical universe, is a remarkable prediction of LQC (see [36–41] and references therein). When $\rho = \rho_{\rm c}$, the Hubble parameter becomes zero, and energy density takes the maximum value ($= \rho_{\rm c}$), so the quantum bounce becomes unalterable. Extensive studies have been conducted on the background evolution with a bounce phase [35, 48, 53, 68–72]. One of the striking features of the quantum bounce is that the desired slow-roll inflation phase is inevitable [61, 62] (also see [16, 23–28, 73–77]).

In the FLRW background, for a potential $V(\phi)$ and single scalar field ϕ the equation of motion in LQC takes the usual form of Klein-Gordon equation as in General Theory of Relativity (GR), given by:

$$\ddot{\phi} + 3H\dot{\phi} + V_{,\phi} = 0, \tag{2.2}$$

[1] This is also true in modified LQCs [47]. For the latter, we refer readers to [63, 64] and references therein.

where $V_{,\phi} = dV(\phi)/d\phi$.

Here, we will study the "pre-inflationary" and "slow-roll inflationary" scenarios for the PLP potential, which has the following form [78]:

$$V(\phi) = V_0 m_{\rm Pl}^4 \left(\frac{\phi^2}{\phi^2 + m^2}\right) , \tag{2.3}$$

where ϕ is the inflaton field and V_0 is the scale of the inflation which can be fixed by matching the amplitude of the scalar power spectrum at the pivot scale of the CMB observations. It is clear that, if m is super-Planckian, then this model becomes indistinguishable from the large field ϕ^n models. Thus, in our analysis, we consider $m = 1$, whereas V_0 is fixed from the recent observation of CMB (elaborately discussed in (III)).

First, we study the background dynamics for inflationary potential given by Eqn. (2.3). By imposing the initial conditions on $a(t)$, $\phi(t)$, and $\dot{\phi}(t)$ at a specific point, one can solve Eqn. (2.1) and Eqn. (2.2) numerically. We set the initial conditions at the bounce $t = t_{\rm B}$, using

$$\frac{1}{2}\dot{\phi}^2(t_{\rm B}) + V(\phi(t_{\rm B})) = \rho_{\rm c}, \quad \text{and} \quad \dot{a}(t_{\rm B}) = 0. \tag{2.4}$$

From now on, the subscript 'B' represents the variable values at the point of the bounce. Considering ρ_c to be a constant and following Eqn. (2.4), one can write $\dot{\phi}_B$ in terms of ρ_c and ϕ_B for a given potential. Thus, one needs to choose the specific initial conditions for $a(t_{\rm B})$ and $\phi(t_{\rm B})$ only. For the sake of simplicity, we choose $a(t)$ by setting the scale factor at bounce, $a(t_{\rm B}) = 1$. Then, the set of initial conditions reduces to only the value of $\phi(t_{\rm B})$. In this analysis, both $\dot{\phi}_{\rm B} > 0$ and $\dot{\phi}_{\rm B} < 0$ cases are considered.

To study the pre-inflationary and inflationary dynamics for the given potential, one needs to introduce a few background quantities such as:

- The equation of state ($\omega(\phi)$), defined as:

$$\omega(\phi) \equiv \frac{\dot{\phi}^2/2 - V(\phi)}{\dot{\phi}^2/2 + V(\phi)}. \tag{2.5}$$

  For the slow-roll inflation, one requires $\omega(\phi) \simeq -1$.

- The first slow-roll parameter (ϵ_H), defined as:

$$\epsilon_H \equiv -\frac{\dot{H}}{H^2}. \tag{2.6}$$

  During the slow-roll inflation, ϵ_H is required to be very small. In standard inflationary scenarios to satisfy the current observation bound on tensor to scalar ratio(r), its required value is about, $\epsilon_H \approx 10^{-3}$.

- The duration of the slow-roll inflation is given in terms of number of e-folds ($N_{\rm inf}$), which represents the amount of the expansion the universe goes from the horizon exit to the end of inflation. It is defined as:

$$N_{\rm inf} \equiv \ln\left(\frac{a_{\rm end}}{a_i}\right). \tag{2.7}$$

  When, $\ddot{a}(t_i) = 0$, i.e., $\ddot{a}(t)$ first changes its sign right after the bouncing phase, defines the starting of the inflation, whereas the inflationary phase ends at $\omega(\phi) \simeq -1/3$.

A. Analytical Evolution of the Background

Background evolution in LQC can be divided universally into three different phases: bouncing, transition, and slow-roll inflationary phase [48, 68–72]. First, we will present the analytic solutions of the scale factor ($a(t)$) near the bouncing phase. Near the bounce phase, kinetic energy is the dominant one, thus the potential term can be ignored. Then Eqn. (2.1) can be rewritten as [48]:

$$H^2 = \frac{8\pi}{3m_{\rm Pl}^2}\frac{1}{2}\dot{\phi}^2\left(1 - \frac{\dot{\phi}^2}{2\rho_{\rm c}}\right), \tag{2.8}$$

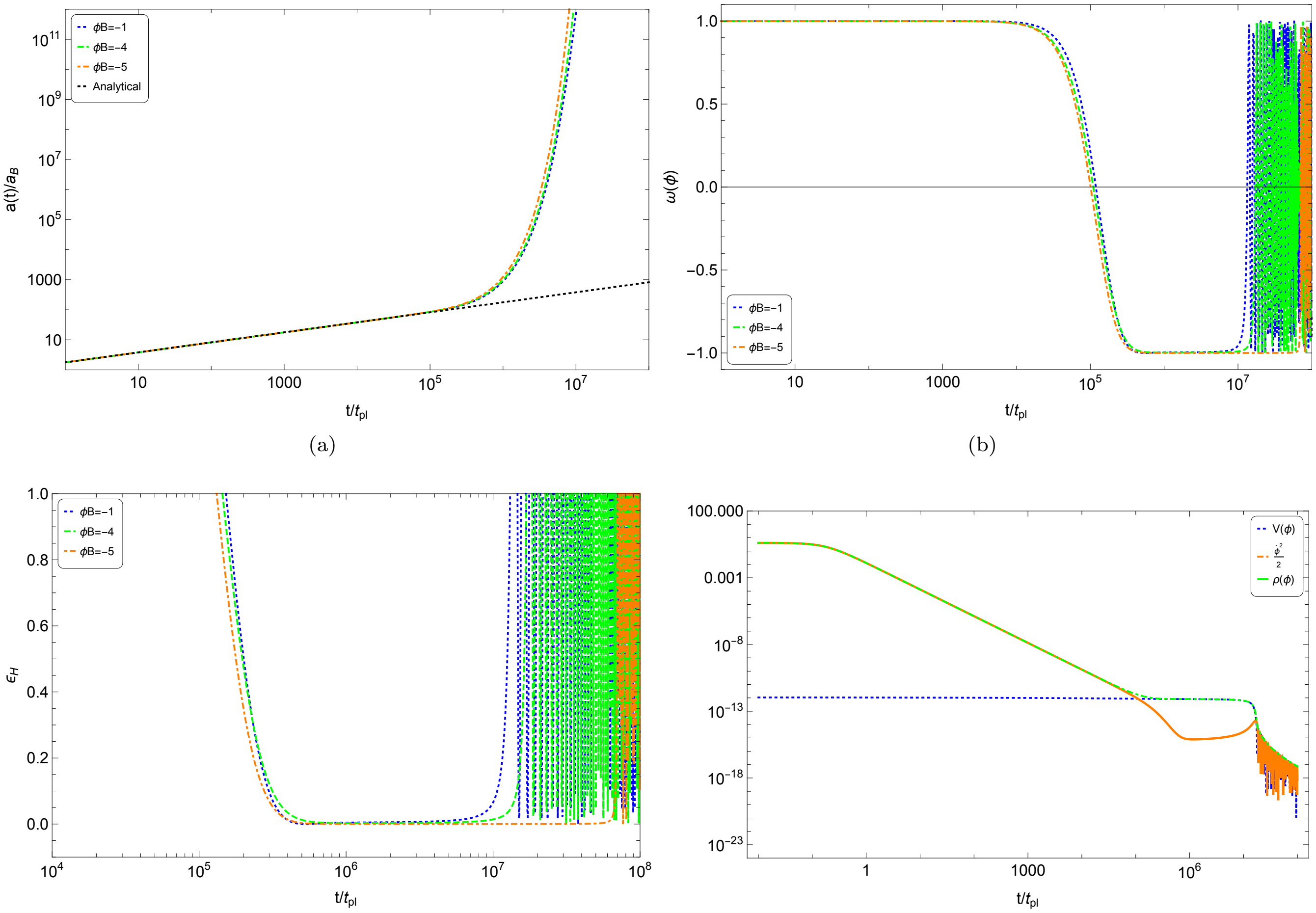

(a) (b) (c) (d)

FIG. 1. Numerical Evolution of the background quantities for the potential (2.3), for the kinetic energy dominated at bounce with $\dot{\phi} > 0$. Fig. 1(a) represents the evolution of the scale factor $a(t)$ for the different initial values of the field ϕ at the bounce. The black dotted line is the representative of the analytical solution. Fig. 1(b) shows the evolution of the equation of state $(\omega(\phi))$ parameter for the different initial values of the ϕ. In Fig. 1(c) we show the solution for the first slow roll parameter (ϵ_H) and in Fig. 1(d) shows the comparison between the potential $V(\phi)$, kinetic energy density $\dot{\phi}^2/2$ along with the total energy density $\rho = \dot{\phi}^2/2 + V(\phi)$, here we take the initial filed value to be $\phi_B = -4$ keeping $\dot{\phi} > 0$.

while the field evolution Eqn. (2.2) now becomes:

$$\ddot{\phi} + 3H\dot{\phi} = 0. \tag{2.9}$$

Solving the above two equations analytically gives:

$$\dot{\phi}(t) = \pm\sqrt{2\rho_{\rm c}}\left(\frac{a_{\rm B}}{a(t)}\right)^3. \tag{2.10}$$

Finally, using Eq. (2.8) and (2.10), the expression of the scale factor$(a(t))$ can be calculated to be:

$$a(t) = a_{\rm B}\left(1 + \gamma_{\rm B}\frac{t^2}{t_{\rm Pl}^2}\right)^{1/6}, \tag{2.11}$$

where $\gamma_{\rm B} \equiv 24\pi\rho_{\rm c}/m_{\rm Pl}^4 \simeq 30.9$ is a dimensionless constant.

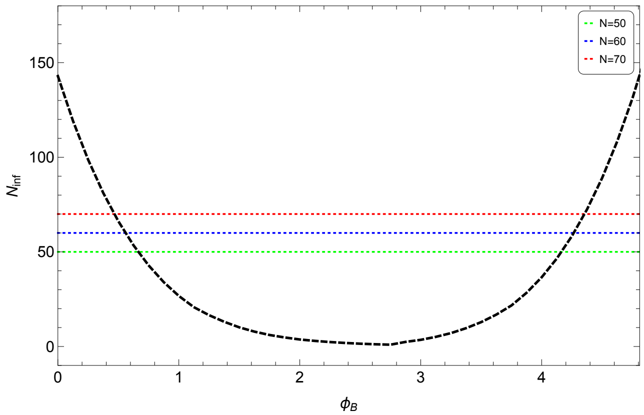

(a)

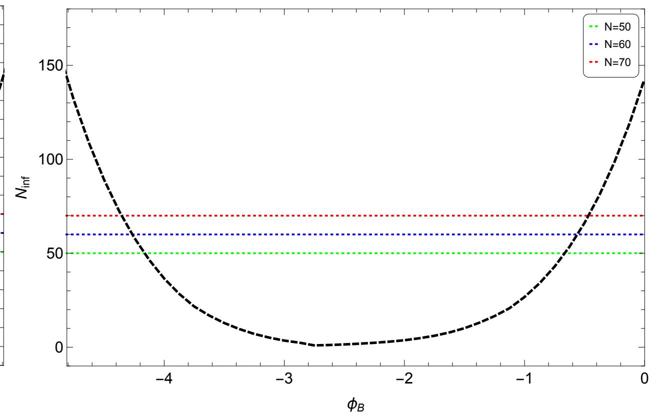

(b)

FIG. 2. Evolution of e-folds for the slow roll inflation against the different choices of ϕ_B. In the left panel, we have considered $\dot{\phi} < 0$ whereas in the right panel, we consider $\dot{\phi} > 0$. Three horizontal dotted lines green, blue, and red denote the $N_{\rm inf} = 50, 60$, and 70 respectively.

B. Numerical evolution of the Background

In this section, we will present the numerical evolution of the background quantities for the different initial field values (ϕ_B). As already mentioned we are setting initial conditions at the time of bounce. The difference in the analytical and numerical evolution can be seen clearly in Fig. 1(a). We carried out the numerical evolution of the background quantities for two different cases, (1) $\phi_B < 0$ and $\dot{\phi} > 0$, and (2) $\phi_B > 0$ and $\dot{\phi} < 0$. Interestingly, due to the intrinsic symmetry of the PLP potential, both cases end up with similar results.

The numerical evolution shown in Fig. 1 for $\dot{\phi}_B > 0$ and different background quantities allows us to extend our understanding of the three different phases: bouncing, transition, and slow roll inflation. From Fig. 1(a) and 1(b) one can see the behavior of the scale factor and the equation of state parameter from the time of the bounce to the inflation. The exponential expansion required for the slow roll inflation is explicitly demonstrated. Around the bounce point, kinetic energy dominates, leading to the equation of state, $\omega = 1$. However, once the kinetic-energy dominates at the bounce, it will dominate for a long time $[t \in (0, 10^5\ t_{Pl})]$ and after that, it starts to decrease dramatically and quickly reaches the point where $\omega = -1$, whereby the slow-roll inflation begins. The end of the inflationary phase is achieved when $\omega \simeq -1/3$ at which we have $\epsilon_H \simeq 1$, as shown in Fig. 3(c). The brief period for ω from 1 to -1 is known as the transition phase. On the other hand, from Fig. 3(d) we can see that the potential energy $V(\phi)$ remains almost constant during the bouncing, transition and slow-roll inflation phases. The slow-roll inflation does not start until the kinetic energy of the inflaton decreases below the potential energy. After a short period of the rapidly exponential expansion, the potential energy drops dramatically, and the inflation ends when it is about equal to the kinetic energy of the inflaton. The e-folds of the expansion of the universe during this epoch depends on the initial conditions ϕ_B, as shown in Fig. 2.

In Fig. 3, we show the numerical solution of the background quantities for $\dot{\phi} < 0$. One can notice that both results are similar and this is attributed to the symmetry in the potential around the minima. A common feature that can be noticed from Figs. 1 - 3 is that the potential energy remains almost constant during the bounce, transition, and inflationary phases. On the other hand, bounce is dominated by kinetic energy which is around the Planck scale and drops down to a value of 12 orders of magnitude below before the onset of the slow roll inflationary epoch.

III. THE SLOW-ROLL INFLATIONARY EPOCH

After the bounce followed by the transition period, the slow roll inflationary phase begins as $\omega \approx -1$. In this period the potential energy starts to dominate over the kinetic energy. At this time, sufficiently far away from the bounce, all LQC effects become negligible during this epoch. The modified Friedmann equation and the scalar field equation of motion take the usual form [3, 79].

$$H^2 \simeq \frac{8\pi}{3m_{\rm Pl}^2} V(\phi), \tag{3.1}$$

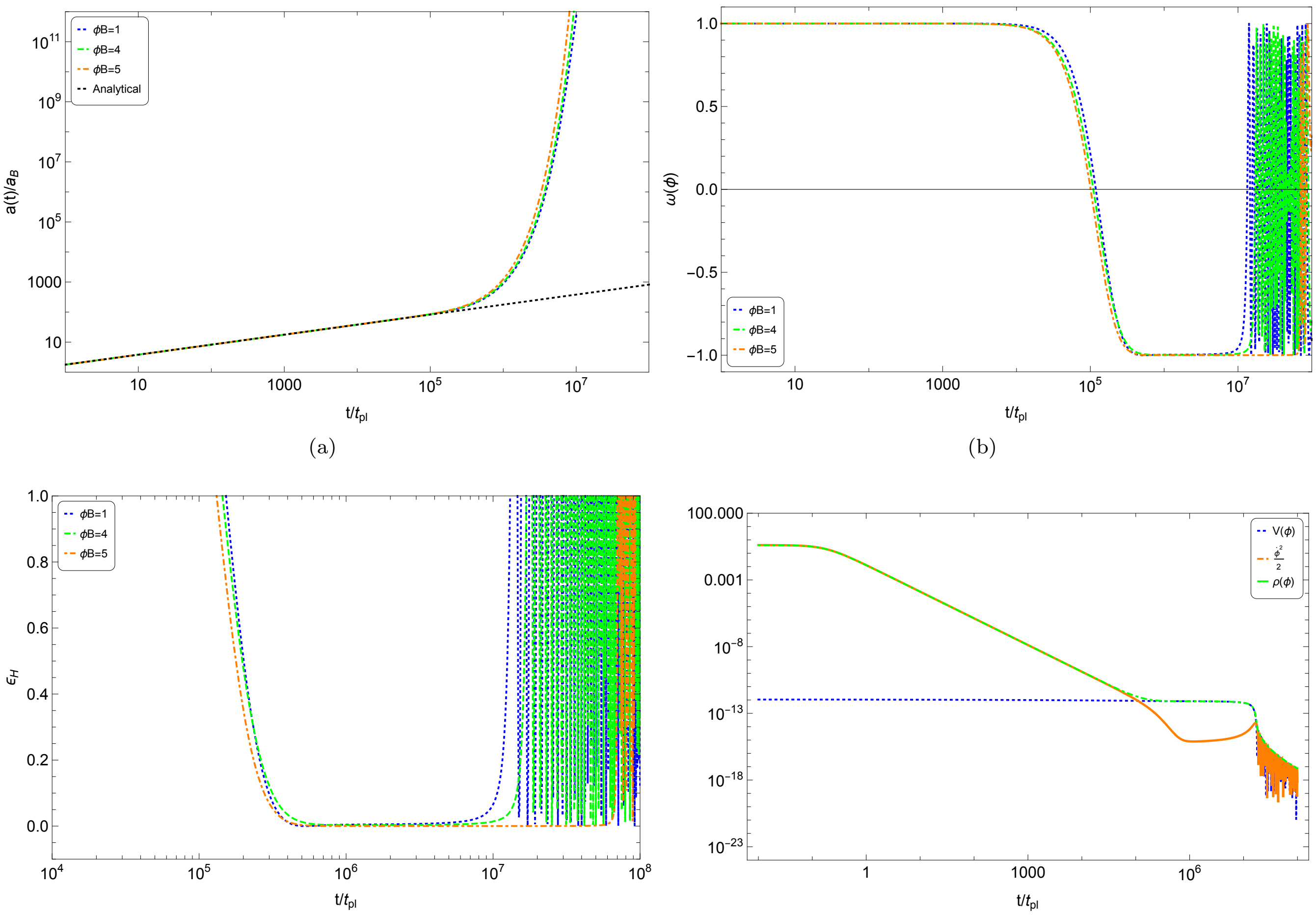

(a) (b) (c) (d)

FIG. 3. Numerical Evolution of the background quantities for the potential (2.3), for the kinetic energy dominated at bounce with $\dot{\phi} < 0$. Fig 3(a) represents the evolution of the scale factor $a(t)$ for the different initial values of the field ϕ. The black dotted is for the analytical solution. Fig 3(b) shows the evolution of the equation of state $(\omega(\phi))$ parameter for the different initial values of the ϕ. In fig 3(c) we show the solution for the first slow roll parameter (ϵ_H) and in fig 3(d) shows the comparison between the potential $V(\phi)$, kinetic energy density $\dot{\phi}^2/2$ along with the total energy density $\rho = \dot{\phi}^2/2 + V(\phi)$, here we take the initial filed value to be $\phi_B = 4$ keeping $\dot{\phi} < 0$.

$$3H\dot{\phi} + \frac{dV(\phi)}{d\phi} \simeq 0. \tag{3.2}$$

With the assumptions, $\frac{1}{2}\dot{\phi}^2 \ll V(\phi), |\ddot{\phi}| \ll |H\dot{\phi}|$. Using the Friedmann equation for the potential $V(\phi)$ one gets:

$$a(t) \propto e^{H_{\rm inf} t}, \tag{3.3}$$

where $H_{\rm inf}$ represents the Hubble parameter during the slow-roll inflation. Using the standard definition of the e-folds $N_{\rm inf}$ in terms of scale factor $a(t)$ along with slow roll conditions, one can express the $N_{\rm inf}$ in terms of the potential:

$$\begin{aligned} N_{\rm inf} &\equiv \ln\left(\frac{a_{\rm end}}{a_i}\right) = \int_{t_i}^{t_{\rm end}} H(t)dt \\ &= \int_{\phi_i}^{\phi_{\rm end}} \frac{H}{\dot{\phi}} d\phi \simeq \frac{8\pi}{m_{\rm Pl}^2} \int_{\phi_{\rm end}}^{\phi_i} \frac{V}{V_\phi} d\phi. \end{aligned} \tag{3.4}$$

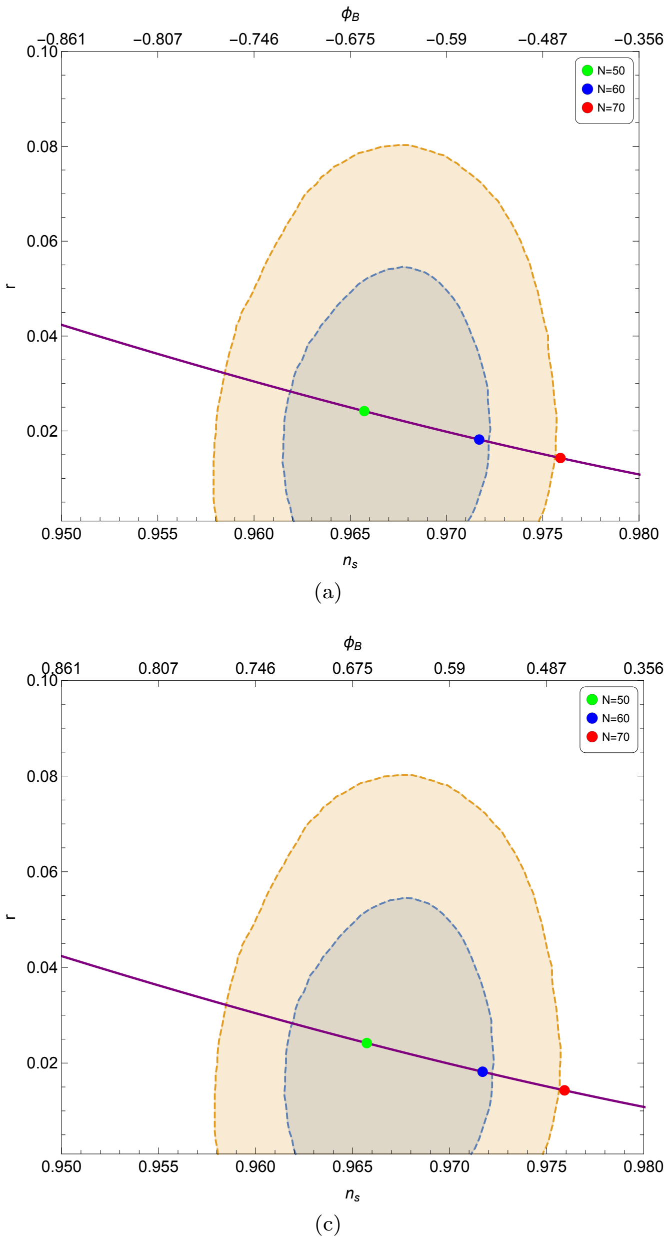

FIG. 4. Figure for $r - n_s$ with the different number of e-fold during the inflation, color green, blue, and red denotes the $50, 60$ and 70 along with the initial field value ϕ_B at the bounce. Two contours blue and light yellow signifies the *Planck'18* $1-\sigma$ and $2-\sigma$ bounds. Fig 4(a), 4(b)represents for the case when $\dot{\phi} > 0$ and fig 4(c),4(d) for the case when $\dot{\phi} < 0$.

Here ϕ_i and ϕ_{end} denote the field value at the onset of inflation and end of inflation respectively. The two slow roll parameters ϵ and η are given in terms of the potential (see [3, 79, 80]),

$$\epsilon = \frac{m_{\rm Pl}^2}{16\pi}\left(\frac{V'(\phi)}{V(\phi)}\right)^2, \qquad \eta = \frac{m_{\rm Pl}^2}{8\pi}\left(\frac{V''(\phi)}{V(\phi)}\right). \tag{3.5}$$

Field values at the end of inflation can be calculated using the end of inflation condition, *i.e.*, $\epsilon = 1$. For any inflationary model to be consistent with recent CMB observation, it needs to satisfy the bounds on a few important quantities as the tensor-to-scalar ratio (r), spectral index (n_s), and scalar power spectrum (A_s), which are defined as:

$$r = 16\epsilon\,, \quad n_s = 1 - 6\epsilon + 2\eta, \quad A_s = \frac{128\pi}{3m_{\rm Pl}^6}\frac{V^3}{V_{,\phi}^2}. \tag{3.6}$$

The explicit expressions for the slow-roll parameters, e-folds and inflationary observable for our model can be expressed (keeping $m_{\rm Pl}=1$)[2]:

$$\epsilon = \frac{1}{4\pi\left(\phi+\phi^3\right)^2}, \qquad \eta = \frac{\left(1-3\phi^2\right)}{4\pi\left(\phi+\phi^3\right)^2}, \qquad N_{\rm inf} \simeq 8\pi \int_{\phi_{\rm end}}^{\phi_i} \frac{1}{2}\phi\left(1+\phi^2\right) d\phi, \tag{3.7}$$

$$r = \frac{4}{\pi\left(\phi+\phi^3\right)^2}, \qquad n_s = 1 - \frac{3}{2\pi\left(\phi+\phi^3\right)^2} + \frac{1-3\phi^2}{2\pi\left(\phi+\phi^3\right)^2}, \qquad A_s = \frac{32\pi V_0 \phi^4\left(1+\phi^2\right)}{3}. \tag{3.8}$$

We calculate all the inflationary observables at the time of horizon exit (start of inflation). It can be seen from Fig. 4 that Our model is consistent with recent CMB observations. For $N=50$ results are well inside the $1-\sigma$ and for $N=60$ results are consistent with the $2-\sigma$ bound. From Planck 2018 observations we found that $A_s \approx 2.09\times10^{-9}$, which allows us to fix the potential parameter V_0 and is about 1.15×10^{-12}. Eq. (3.4) allows us to calculate the field value at the time of the horizon exit for a given number of the e-fold. Using this fact along with the relation between $N_{\rm inf}$ and ϕ_B as depicted in Fig. 2, we manage to establish the relation between n_s and ϕ_B which has been shown in Fig. 4, which can be used to directly constrain the initial value of ϕ_B, in order to be consistent with observations.

IV. REHEATING ANALYSIS

One of the inevitable epoch to follow the inflationary paradigm is reheating [81–83], where the inflaton field transfers its energy to other degrees of freedom and resurrects the universe from super-cooled state to a hot thermal bath of relativistic particles. The idea of reheating was first proposed in [82]. In the standard inflationary scenario, numerous methods of reheating have been proposed in the literature such as perturbative decay where the inflaton field reaches the bottom of the potential and starts to decay to other elementary particlesv [84–87]. The produced particles interact each other and reach an equilibrium at a temperature known as reheating temperature (T_{re}). There are other theoretically interesting methods that were introduced later, such as parametric resonance, which is a non-perturbative method, tachyonic instability [88], and preheating [89, 90]. The initial stage of the reheating can be attributed to the preheating phase. Preheating is more efficient as compared to perturbative reheating. In preheating the decay happens exponentially generating the high number of particles.

However, the epoch of reheating can be studied in great detail without delving deep into the microphysical dynamics of this phase [91]. As there is no direct observational bound on the reheating temperature, analysis of this era in an indirect approach can be extremely useful. In this approach, one can give a bound on the thermalization temperature through the inflationary observables. Moreover, such approaches can be used as a new way to constrain different inflationary models. Along with the reheating temperature (T_{re}) and the equation of state parameter (ω_{re}), another important physical quantity is the duration of reheating dubbed as the number of e-folds (N_{re}) during the reheating. N_{re} quantifies the expansion of the universe from the end of inflation to the end of the thermalization period. Following [91–95] reheating temperature (T_{re}) and duration of the reheating (N_{re}) can be written in terms of the effective equation of state (ω_{re}) as:

$$N_{re} = \frac{4}{(1-3w_{re})}\left[61.48 - \ln\left(\frac{V_{end}^{\frac{1}{4}}}{H_k}\right) - N_k\right] \tag{4.1}$$

$$T_{re} = \left[\left(\frac{43}{11 g_{re}}\right)^{\frac{1}{3}} \frac{a_0 T_0}{k} H_k e^{-N_k}\left[\frac{3^2\cdot 5 V_{end}}{\pi^2 g_{re}}\right]^{-\frac{1}{3(1+w_{re})}}\right]^{\frac{3(1+w_{re})}{3w_{re}-1}}. \tag{4.2}$$

Here g_{re} is the relativistic degree of freedom, a_0 and T_0 denote the present value of scale factor and temperature, respectively, while k signifies the *Planck's* pivot scale. H_k represents the Hubble parameter and V_{end} is the potential at the end of inflation. The number of e-folds during the inflation is defined as N_k. The Hubble parameter can be written in terms of inflationary observables as:

$$H_k = \frac{1}{4}\left(\pi r A_s\right)^{1/2}. \tag{4.3}$$

[2] For the reminder of the paper, we have kept $m_{\rm Pl}=1$.

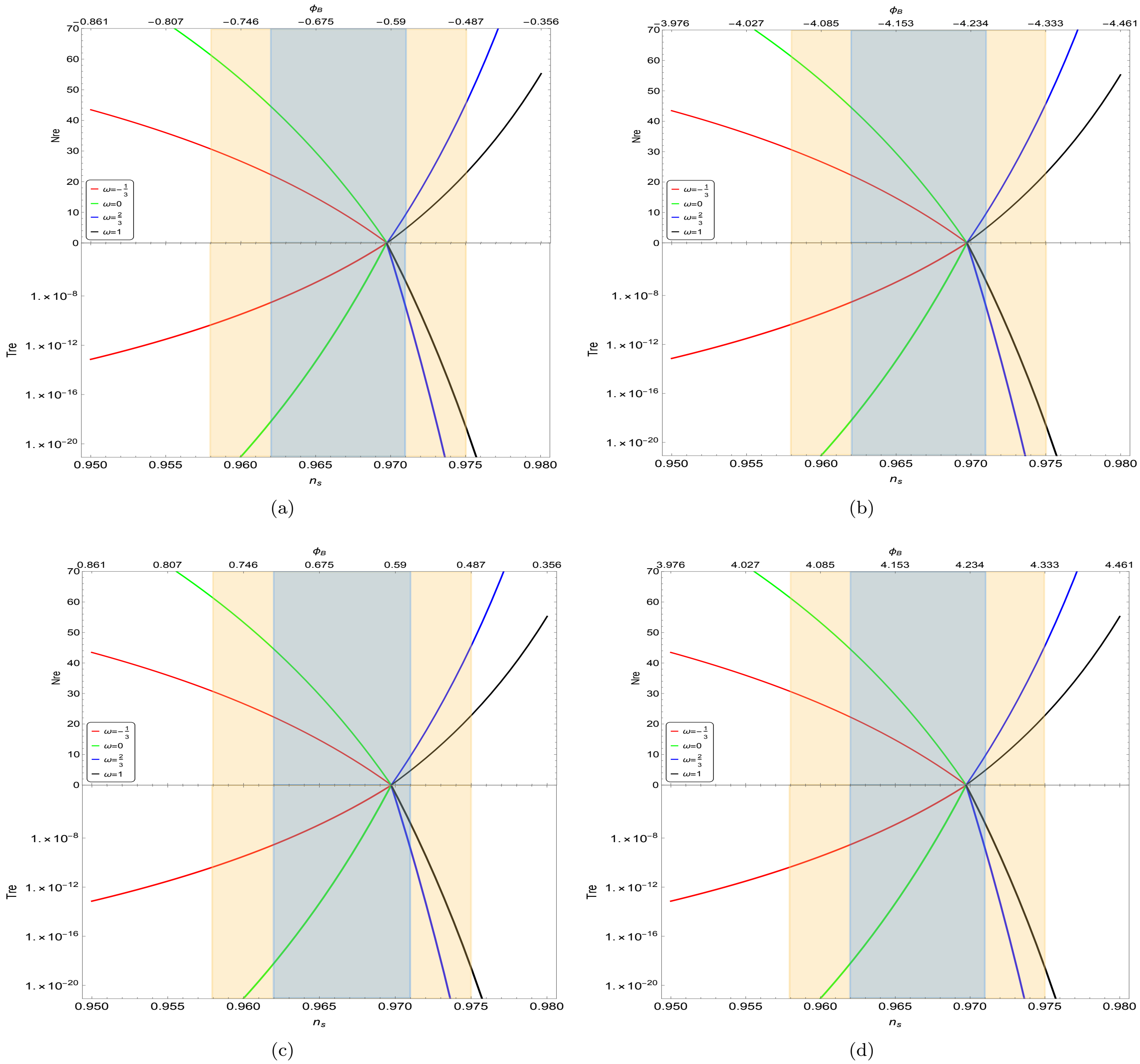

FIG. 5. Plot for the number of e-folds N_{re} and reheating temperature T_{re} during the reheating phase for the different equation of state parameter (ω_{re}). The light yellow and blue shaded region represents *Planck'18*, $2-\sigma$ and $1-\sigma$ constraints on n_s. Different color signifies the different values of ω_{re} as mentioned in the plot. Fig. 5(b), 5(a) for the case when $\dot{\phi} > 0$ and 5(c), 5(d) when $\dot{\phi} < 0$.

Maintaining $A_s(k_0) = 2.09\times10^{-9}$ (variation of A_s has a negligible effect on T_{re} and N_{re}), the rest of the calculations are carried strainghtforward. It is evident from Eqn. (4.1) and Eqn. (4.2) that both equations depend on H_k. From Eq.(4.3), it's clear that H_k is a function of the tensor to scalar ratio (r). We write r in terms of scalar spectral index (n_s) which would help us to constraint T_{re} and N_{re} more accurately. From $\epsilon = 1$ as the end of inflation, we can calculate V_{end}, equipped with all the preliminaries now we can calculate T_{re} and N_{re} for different equations of state (ω_{re}). The results for the reheating analysis can be found in Fig. 5. We have considered four different values of ($\omega_{re} = -1/3, 0, 2/3, 1$), however, one can easily extend the calculations for other values of ω_{re}. Color red, green, blue, and black signify the different ω_{re} as mentioned in Fig. 5. The light yellow and blue shaded region represents *Planck 2018*, $2-\sigma$ and $1-\sigma$ constraints on n_s. In Fig. 5 we have plotted the T_{re} from the scale of instantaneous reheating to the the Big Bang Nucleosynthesis (BBN), which is around 10Mev. The point where all the curves in N_{re} and T_{re}

mergers represent the scale of instantaneous reheating ($N_{re} = 0$). As our inflationary model, PLP has an origination from supersymmetric theory, and g_{re} is taken to be 226 for the rest of the calculation.

V. REHEATING AND EXPANSION HISTORY

In this section, we will present the main results of our analysis. The total expansion of the universe from the point of bounce till today (N_T) can be expressed in terms of the scale factor as:

$$N_T = \ln\left(\frac{a_0}{a_B}\right) \quad = \ln\left(\frac{a_i}{a_B}\cdot\frac{a_{end}}{a_i}\cdot\frac{a_{re}}{a_{end}}\cdot\frac{a_0}{a_{re}}\right), \tag{5.1}$$

where different subscripts in the scale factor define the different eras of the expansion history of the universe. In particular, the subscripts B, i, end, re signify the scale factor at bounce, the onset of inflation, the end of inflation, and the end of reheating, respectively. Whereas the subscript 0 denotes the value of the scale factor today. Eqn. (5.1) can be written more simplistically as:

$$N_T = N_{pre} + N_{inf} + N_{re} + \ln\left(\frac{a_0}{a_{re}}\right). \tag{5.2}$$

Again the subscript defines the number of e-folds during the different epochs. Furthermore, the factor a_0/a_{re} can be defined in terms of the reheating temperature(T_{re}) as:

$$\frac{a_0}{a_{re}} = \left(\frac{11g_{re}}{43}\right)^{\frac{1}{3}}\frac{T_{re}}{T_0} = \left(\frac{11g_{re}}{43}\right)^{\frac{1}{3}}\left[\left(\frac{43}{11g_{re}}\right)^{\frac{1}{3}}\left(\frac{a_0T_0}{k}\right)H_k e^{-N_k}\left[\frac{3^2\cdot 5V_{end}}{\pi^2 g_{re}}\right]^{-\frac{1}{3(1+w_{re})}}\right]^{\frac{3(1+w_{re})}{3w_{re}-1}}\frac{1}{T_0}. \tag{5.3}$$

Substituting the Eqs. (5.3) and (4.1) in Eq. (5.2) one can write the total number of e-folds in terms of the reheating temperature and then in terms of the inflationary variables. As N_{pre} weakly depends on the form of the potential almost all the previous studies suggest $N_{pre} \simeq 4-5$, which is also the case for this model. It is well known that one needs N_{inf} to be in the range of $50-65$, in order to solve the problems of the Big Bang cosmology. One can express N_{inf} in terms of n_s. In our analysis, we are not assuming $N_{re} = 0$ (instantaneous reheating scenario), rather allowed the reheating to be the generalised case. Furthermore, in our analysis N_{re} and T_{re} both can vary to a wide range from instantaneous to the BBN temperature depending on the value of ω_{re} and n_S. This allows us to compute N_T for different values of ω_{re} and n_s. Finally Eqn. (5.2) can be written in combination of ω_{re} and n_s by using Eqs. (4.1) and (4.2).

Our results significantly differs from the previous studies presented in the literature where the $N_T \geq 141$ [16, 48, 96], taking an instantaneous reheating scenario. Whereas, if we consider the generalised reheating scenario, we find that (see Fig. 6)

$$N_T \approx 127. \tag{5.4}$$

It may seem to be counterintuitive, that choosing $N_{re} \neq 0$, N_T goes to a lower value. But, this is due to the fact that, in the previous studies, it was considered that the $N_{\rm pre} + N_{\rm inf} \geq 81$ and $\ln(a_0/a_{re}) \approx 60$. Since, $N_{\rm pre} \simeq 4-5$, then $N_{\rm inf} \geq 76-77$, which from the observational point of view, is very large. Whereas in our current analysis we constrain $N_{\rm inf}, N_{\rm re}, T_{\rm re}$ and N_T from the CMB observations on n_S. In Fig. 6, we have plotted N_T with n_s while the upper horizontal axis shows ϕ_B corresponding to n_s. Using the correspondence between ϕ_B and n_s, one can explicitly calculate $N_{\rm inf}$, $N_{\rm re}$ and $T_{\rm re}$ for different values of $\omega_{\rm re}$ (we keep $N_{\rm pre} \simeq 4-5$).

VI. CONCLUSION

In this paper, for the first time, we have calculated the total number of e-foldings (N_T) in LQC, keeping the reheating epoch to be the realistic generalized one, which means the Universe is allowed to grow few e-folds during reheating rather than taking it to be instantaneous. CMB observations constrain the inflationary parameter such as n_s severely. Thus, N_T is represented as a function of n_s for different ω_{re} as shown in Fig. 6. To successfully analyze inflation and reheating in a supersymmetric model, it's important to address gravitino overproduction. The existence of the gravitino poses significant cosmological issues, potentially jeopardizing the feasibility of BBN. For a successful phase of BBN, $T_{\rm re}$ must be less than 10^8Gev. Due to this fact, in Fig. 6 we have represented N_T for the values of

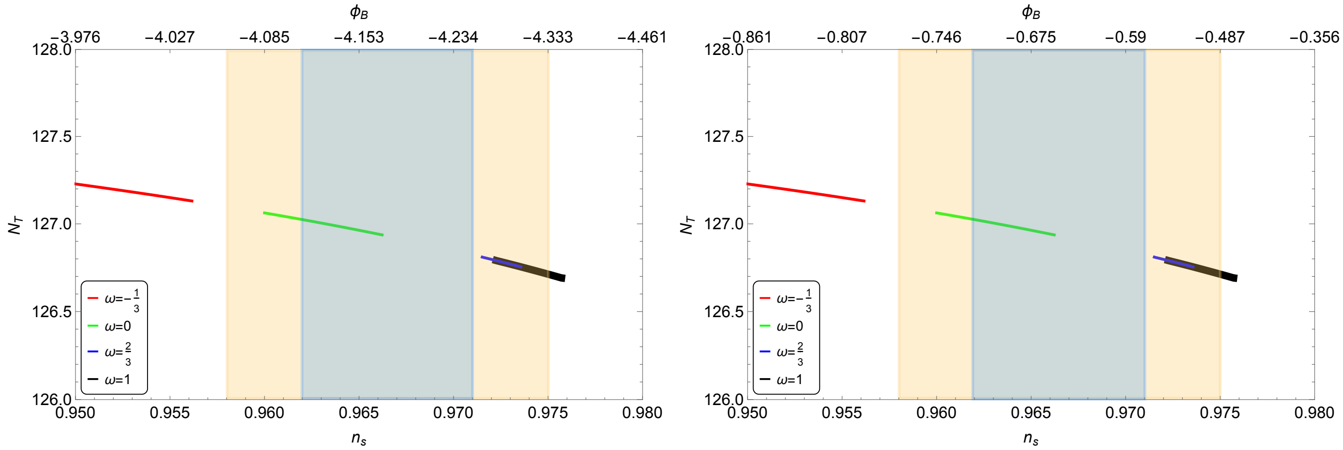

(a) (b)

FIG. 6. Total number of e-folds (N_T) against the scalar spectral index (n_s) for $\dot{\phi} > 0$. The light yellow and blue shaded region represents *Planck'18*, $2-\sigma$ and $1-\sigma$ constraints on n_s. It is straightforward to extend the results for $\dot{\phi} < 0$ case which we are not presenting here.

T_{re} from 10^8Gev to the BBN temperature ($\approx$ 10Mev) for different values of ω_{re}. From Fig. 5 one can see that the limits on the T_{re} to avoid gravitino overproduction results in the constrain on the allowed value of n_s depending on ω_{re}. This leads to the situation where N_T is no longer a continuous function of n_S, which is demonstrated in Fig. 6. In this analysis, the number of e-folds during inflation is constrained by n_s and thus our results give a significantly different value of $N_T \simeq 127$ than the previous studies where $N_T \gtrsim 141$ when the reheating epoch was considered to be instantaneous [16, 48, 96].

As we know that quantum geometric effects are mainly concentrated in the regions near the bounce, and at the time of inflationary pahse we are far away from the bounce and such effects get diluted significantly. On the other hand, the major contributions to N_T come from inflation and reheating whereas N_{pre} is always around $4-5$. Therefore, we expect that our results on $N_T(\approx 127)$ will not change much in modified loop quantum cosmologies, such as mLQC-I and mLQC-II [63, 64].

The studies of this paper open up a new avenue to study the LQC through the indirect investigations of the reheating epoch. On this note, it will be interesting to perform this exercise in cases of well-motivated models of particle physics such as the natural or more generic Goldstone inflation [97–99]. One should also try to explore the effect of LQC on the low ℓ anomaly (explained by resonance particle production in [100, 101]) observed in the CMB power spectrum by [10] for a long time. The pre-inflationary dynamics can introduce interesting features which may explain such anomalies.

Finally, we note that particle productions in LQC are a natural phenomenon, and such studies for a warm inflationary scenario in LQC have already been considered in [57, 102], but studies in the more realistic scenario following [103, 104] is in order. As it has been shown very recently that warm inflation can naturally produce primordial black holes (PBHs) and induced gravitational waves [105, 106], it will be very interesting to investigate the effects of pre-inflationary dynamics in these contexts. The authors would like to come to these questions in future studies.

ACKNOWLEDGEMENT

The authors would like to thank Drs. Bao-Fei Li, Abolhassan Mohammadi and Tao Zhu for fruitful discussions. M.R.G. thanks OMEG Institute, Soongsil University, Republic of Korea, for their hospitality, where the last part of the paper was completed. A.W. thanks the hospitality of the Centre for Cosmology and Science Popularization, SGT University, India, during his visit (November - December 2024), during which the project was initiated.

Work of M.R.G. is supported by the Department of Science and Technology(DST), Government of India under the Grant Agreement number IF18-PH-228 (INSPIRE Faculty Award) and by the Science and Engineering Research Board (SERB), DST, Government of India under the Grant Agreement number CRG/2022/004120 (Core Research

Grant). A.W. is partially supported by the US NSF grant: PHY-2308845.

[1] A. H. Guth, Phys. Rev. D **23**, 347 (1981).
[2] A. A. Starobinsky, Phys. Lett. B **91**, 99 (1980).
[3] D. Baumann, in *Theoretical Advanced Study Institute in Elementary Particle Physics: Physics of the Large and the Small* (2011) pp. 523–686, arXiv:0907.5424 [hep-th].
[4] A. D. Linde, Phys. Lett. B **108**, 389 (1982).
[5] A. D. Linde, Phys. Lett. B **129**, 177 (1983).
[6] A. H. Guth and S. Y. Pi, Phys. Rev. Lett. **49**, 1110 (1982).
[7] E. Komatsu *et al.*, The Astrophysical Journal Supplement Series **192**, 18 (2011).
[8] P. A. R. Ade *et al.* (Planck), Astron. Astrophys. **571**, A22 (2014), arXiv:1303.5082 [astro-ph.CO].
[9] P. A. R. Ade *et al.* (Planck), Astron. Astrophys. **594**, A20 (2016), arXiv:1502.02114 [astro-ph.CO].
[10] Y. Akrami *et al.* (Planck), Astron. Astrophys. **641**, A10 (2020), arXiv:1807.06211 [astro-ph.CO].
[11] J. Martin, C. Ringeval, and V. Vennin, Phys. Dark Univ. **5-6**, 75 (2014), arXiv:1303.3787 [astro-ph.CO].
[12] R. H. Brandenberger and J. Martin, Class. Quant. Grav. **30**, 113001 (2013), arXiv:1211.6753 [astro-ph.CO].
[13] J. Martin and R. H. Brandenberger, Phys. Rev. D **63**, 123501 (2001), arXiv:hep-th/0005209.
[14] A. Borde, A. H. Guth, and A. Vilenkin, Phys. Rev. Lett. **90**, 151301 (2003), arXiv:gr-qc/0110012.
[15] A. Borde and A. Vilenkin, Phys. Rev. Lett. **72**, 3305 (1994), arXiv:gr-qc/9312022.
[16] A. Ashtekar and P. Singh, Class. Quant. Grav. **28**, 213001 (2011), arXiv:1108.0893 [gr-qc].
[17] M. Bojowald, Rept. Prog. Phys. **78**, 023901 (2015), arXiv:1501.04899 [gr-qc].
[18] B.-F. Li and P. Singh, (2023), arXiv:2304.05426 [gr-qc].
[19] A. Ashtekar, W. Kaminski, and J. Lewandowski, Phys. Rev. D **79**, 064030 (2009), arXiv:0901.0933 [gr-qc].
[20] I. Agullo, A. Ashtekar, and W. Nelson, Phys. Rev. Lett. **109**, 251301 (2012), arXiv:1209.1609 [gr-qc].
[21] I. Agullo, A. Ashtekar, and W. Nelson, Phys. Rev. D **87**, 043507 (2013), arXiv:1211.1354 [gr-qc].
[22] I. Agullo, A. Ashtekar, and W. Nelson, Class. Quant. Grav. **30**, 085014 (2013), arXiv:1302.0254 [gr-qc].
[23] M. Bojowald, G. M. Hossain, M. Kagan, and S. Shankaranarayanan, Phys. Rev. D **79**, 043505 (2009), [Erratum: Phys.Rev.D 82, 109903 (2010)], arXiv:0811.1572 [gr-qc].
[24] J. Mielczarek, T. Cailleteau, A. Barrau, and J. Grain, Class. Quant. Grav. **29**, 085009 (2012), arXiv:1106.3744 [gr-qc].
[25] T. Cailleteau, J. Mielczarek, A. Barrau, and J. Grain, Class. Quant. Grav. **29**, 095010 (2012), arXiv:1111.3535 [gr-qc].
[26] T. Cailleteau, A. Barrau, J. Grain, and F. Vidotto, Phys. Rev. D **86**, 087301 (2012), arXiv:1206.6736 [gr-qc].
[27] T. Cailleteau, L. Linsefors, and A. Barrau, Class. Quant. Grav. **31**, 125011 (2014), arXiv:1307.5238 [gr-qc].
[28] A. Barrau, M. Bojowald, G. Calcagni, J. Grain, and M. Kagan, JCAP **05**, 051 (2015), arXiv:1404.1018 [gr-qc].
[29] M. Bojowald, G. Calcagni, and S. Tsujikawa, Phys. Rev. Lett. **107**, 211302 (2011), arXiv:1101.5391 [astro-ph.CO].
[30] M. Bojowald, G. Calcagni, and S. Tsujikawa, JCAP **11**, 046 (2011), arXiv:1107.1540 [gr-qc].
[31] T. Zhu, A. Wang, G. Cleaver, K. Kirsten, Q. Sheng, and Q. Wu, Astrophys. J. Lett. **807**, L17 (2015), arXiv:1503.06761 [gr-qc].
[32] T. Zhu, A. Wang, G. Cleaver, K. Kirsten, Q. Sheng, and Q. Wu, JCAP **10**, 052 (2015), arXiv:1508.03239 [gr-qc].
[33] T. Zhu, A. Wang, K. Kirsten, G. Cleaver, Q. Sheng, and Q. Wu, JCAP **03**, 046 (2016), arXiv:1510.03855 [gr-qc].
[34] B. Bonga and B. Gupt, Gen. Rel. Grav. **48**, 71 (2016), arXiv:1510.00680 [gr-qc].
[35] B. Bonga and B. Gupt, Phys. Rev. D **93**, 063513 (2016), arXiv:1510.04896 [gr-qc].
[36] M. Bojowald, Phys. Rev. Lett. **86**, 5227 (2001), arXiv:gr-qc/0102069.
[37] A. Ashtekar, T. Pawlowski, and P. Singh, Phys. Rev. Lett. **96**, 141301 (2006), arXiv:gr-qc/0602086.
[38] A. Ashtekar, T. Pawlowski, and P. Singh, Phys. Rev. D **73**, 124038 (2006), arXiv:gr-qc/0604013.
[39] A. Ashtekar, T. Pawlowski, and P. Singh, Phys. Rev. D **74**, 084003 (2006), arXiv:gr-qc/0607039.
[40] A. Ashtekar, A. Corichi, and P. Singh, Phys. Rev. D **77**, 024046 (2008), arXiv:0710.3565 [gr-qc].
[41] J. Yang, Y. Ding, and Y. Ma, Phys. Lett. B **682**, 1 (2009), arXiv:0904.4379 [gr-qc].
[42] B.-F. Li, S. Saini, and P. Singh, Phys. Rev. D **103**, 066020 (2021), arXiv:2012.10462 [gr-qc].
[43] B.-F. Li, J. Olmedo, P. Singh, and A. Wang, Phys. Rev. D **102**, 126025 (2020), arXiv:2008.09135 [gr-qc].
[44] B.-F. Li, P. Singh, and A. Wang, Phys. Rev. D **101**, 086004 (2020), arXiv:1912.08225 [gr-qc].
[45] B.-F. Li, P. Singh, and A. Wang, Phys. Rev. D **98**, 066016 (2018), arXiv:1807.05236 [gr-qc].
[46] B.-F. Li, P. Singh, and A. Wang, Phys. Rev. D **97**, 084029 (2018), arXiv:1801.07313 [gr-qc].
[47] B.-F. Li, P. Singh, and A. Wang, Phys. Rev. D **100**, 063513 (2019), arXiv:1906.01001 [gr-qc].
[48] T. Zhu, A. Wang, G. Cleaver, K. Kirsten, and Q. Sheng, Phys. Rev. D **96**, 083520 (2017), arXiv:1705.07544 [gr-qc].
[49] T. Zhu, A. Wang, K. Kirsten, G. Cleaver, and Q. Sheng, Phys. Lett. B **773**, 196 (2017), arXiv:1607.06329 [gr-qc].
[50] B.-F. Li, T. Zhu, A. Wang, K. Kirsten, G. Cleaver, and Q. Sheng, Phys. Rev. D **99**, 103536 (2019), arXiv:1812.11191 [gr-qc].
[51] J. Qiao, G.-H. Ding, Q. Wu, T. Zhu, and A. Wang, JCAP **09**, 064 (2019), arXiv:1811.03216 [hep-th].
[52] I. Agullo, A. Wang, and E. Wilson-Ewing, "Loop quantum cosmology: Relation between theory and observations," in *Handbook of Quantum Gravity*, edited by C. Bambi, L. Modesto, and I. Shapiro (Springer Nature Singapore, Singapore, 2023) pp. 1–46.

[53] G. L. L. W. Levy and R. O. Ramos, (2024), arXiv:2404.10149 [gr-qc].
[54] L. N. Barboza, G. L. L. W. Levy, L. L. Graef, and R. O. Ramos, Phys. Rev. D **106**, 103535 (2022), arXiv:2206.14881 [gr-qc].
[55] L. N. Barboza, L. L. Graef, and R. O. Ramos, Phys. Rev. D **102**, 103521 (2020), arXiv:2009.13587 [gr-qc].
[56] A. Mohammadi, (2024), arXiv:2403.18289 [gr-qc].
[57] L. L. Graef and R. O. Ramos, Phys. Rev. D **98**, 023531 (2018), arXiv:1805.05985 [gr-qc].
[58] L. L. Graef, R. O. Ramos, and G. S. Vicente, Phys. Rev. D **102**, 043518 (2020), arXiv:2007.02395 [gr-qc].
[59] I. Agullo and P. Singh, "Loop Quantum Cosmology," in *Loop Quantum Gravity: The First 30 Years*, edited by A. Ashtekar and J. Pullin (WSP, 2017) pp. 183–240, arXiv:1612.01236 [gr-qc].
[60] A. Ashtekar and J. Pullin, (2017), arXiv:1703.07396 [gr-qc].
[61] A. Ashtekar and D. Sloan, Phys. Lett. B **694**, 108 (2011), arXiv:0912.4093 [gr-qc].
[62] A. Ashtekar and D. Sloan, Gen. Rel. Grav. **43**, 3619 (2011), arXiv:1103.2475 [gr-qc].
[63] B.-F. Li, P. Singh, and A. Wang, Front. Astron. Space Sci. **8**, 701417 (2021), arXiv:2105.14067 [gr-qc].
[64] J. Saeed, R. Pan, C. Brown, G. Clevear, and A. Wang, (2024), arXiv:2406.06745 [gr-qc].
[65] V. Taveras, Phys. Rev. D **78**, 064072 (2008), arXiv:0807.3325 [gr-qc].
[66] M. Bojowald and A. Skirzewski, Rev. Math. Phys. **18**, 713 (2006), arXiv:math-ph/0511043.
[67] M. Bojowald, B. Sandhofer, A. Skirzewski, and A. Tsobanjan, Rev. Math. Phys. **21**, 111 (2009), arXiv:0804.3365 [math-ph].
[68] M. Shahalam, M. Sharma, Q. Wu, and A. Wang, Phys. Rev. D **96**, 123533 (2017), arXiv:1710.09845 [gr-qc].
[69] M. Shahalam, M. Sami, and A. Wang, Phys. Rev. D **98**, 043524 (2018), arXiv:1806.05815 [astro-ph.CO].
[70] M. Sharma, M. Shahalam, Q. Wu, and A. Wang, JCAP **11**, 003 (2018), arXiv:1808.05134 [gr-qc].
[71] M. Sharma, T. Zhu, and A. Wang, Commun. Theor. Phys. **71**, 1205 (2019), arXiv:1903.07382 [gr-qc].
[72] M. Shahalam, M. Al Ajmi, R. Myrzakulov, and A. Wang, Class. Quant. Grav. **37**, 195026 (2020), arXiv:1912.00616 [gr-qc].
[73] A. Ashtekar and B. Gupt, Class. Quant. Grav. **34**, 014002 (2017), arXiv:1608.04228 [gr-qc].
[74] P. Singh, K. Vandersloot, and G. V. Vereshchagin, Phys. Rev. D **74**, 043510 (2006), arXiv:gr-qc/0606032.
[75] J. Mielczarek, T. Cailleteau, J. Grain, and A. Barrau, Phys. Rev. D **81**, 104049 (2010), arXiv:1003.4660 [gr-qc].
[76] X. Zhang and Y. Ling, JCAP **08**, 012 (2007), arXiv:0705.2656 [gr-qc].
[77] L. Chen and J.-Y. Zhu, Phys. Rev. D **92**, 084063 (2015), arXiv:1510.03135 [gr-qc].
[78] K. Dimopoulos and C. Owen, Phys. Rev. D **94**, 063518 (2016), arXiv:1607.02469 [hep-ph].
[79] A. R. Liddle, P. Parsons, and J. D. Barrow, Phys. Rev. D **50**, 7222 (1994), arXiv:astro-ph/9408015.
[80] A. Riotto, ICTP Lect. Notes Ser. **14**, 317 (2003), arXiv:hep-ph/0210162.
[81] A. Albrecht, P. J. Steinhardt, M. S. Turner, and F. Wilczek, Phys. Rev. Lett. **48**, 1437 (1982).
[82] L. Kofman, A. D. Linde, and A. A. Starobinsky, Phys. Rev. Lett. **73**, 3195 (1994), arXiv:hep-th/9405187.
[83] J. Martin, C. Ringeval, and V. Vennin, Phys. Rev. Lett. **114**, 081303 (2015), arXiv:1410.7958 [astro-ph.CO].
[84] L. Kofman, A. D. Linde, and A. A. Starobinsky, Phys. Rev. D **56**, 3258 (1997), arXiv:hep-ph/9704452.
[85] Y. Shtanov, J. H. Traschen, and R. H. Brandenberger, Phys. Rev. D **51**, 5438 (1995), arXiv:hep-ph/9407247.
[86] B. A. Bassett, S. Tsujikawa, and D. Wands, Rev. Mod. Phys. **78**, 537 (2006), arXiv:astro-ph/0507632.
[87] T. Rehagen and G. B. Gelmini, JCAP **06**, 039 (2015), arXiv:1504.03768 [hep-ph].
[88] G. N. Felder, L. Kofman, and A. D. Linde, Phys. Rev. D **64**, 123517 (2001), arXiv:hep-th/0106179.
[89] K. D. Lozanov, (2019), arXiv:1907.04402 [astro-ph.CO].
[90] L. Kofman, in *3rd RESCEU International Symposium on Particle Cosmology* (1997) pp. 1–8, arXiv:hep-ph/9802285.
[91] J. L. Cook, E. Dimastrogiovanni, D. A. Easson, and L. M. Krauss, JCAP **04**, 047 (2015), arXiv:1502.04673 [astro-ph.CO].
[92] S. Bhattacharya, K. Das, and M. R. Gangopadhyay, Class. Quant. Grav. **37**, 215009 (2020), arXiv:1908.02542 [astro-ph.CO].
[93] H. A. Khan and Yogesh, Phys. Rev. D **105**, 063526 (2022), arXiv:2201.06439 [astro-ph.CO].
[94] M. R. Gangopadhyay, H. A. Khan, and Yogesh, Phys. Dark Univ. **40**, 101177 (2023), arXiv:2205.15261 [astro-ph.CO].
[95] R. Adhikari, M. R. Gangopadhyay, and Yogesh, Grav. Cosmol. **28**, 1 (2022), arXiv:1909.07217 [astro-ph.CO].
[96] Q. Wu, T. Zhu, and A. Wang, Phys. Rev. D **98**, 103528 (2018), arXiv:1809.03172 [gr-qc].
[97] K. Freese, J. A. Frieman, and A. V. Olinto, Phys. Rev. Lett. **65**, 3233 (1990).
[98] D. Croon, V. Sanz, and J. Setford, JHEP **10**, 020 (2015), arXiv:1503.08097 [hep-ph].
[99] S. Bhattacharya and M. R. Gangopadhyay, Phys. Rev. D **101**, 023509 (2020), arXiv:1812.08141 [astro-ph.CO].
[100] G. J. Mathews, M. R. Gangopadhyay, K. Ichiki, and T. Kajino, Phys. Rev. D **92**, 123519 (2015), arXiv:1504.06913 [astro-ph.CO].
[101] M. R. Gangopadhyay, G. J. Mathews, K. Ichiki, and T. Kajino, Eur. Phys. J. C **78**, 733 (2018), arXiv:1701.00577 [astro-ph.CO].
[102] M. Benetti, L. Graef, and R. O. Ramos, JCAP **10**, 066 (2019), arXiv:1907.03633 [astro-ph.CO].
[103] M. Bastero-Gil, A. Berera, R. O. Ramos, and J. G. Rosa, Phys. Rev. Lett. **117**, 151301 (2016), arXiv:1604.08838 [hep-ph].
[104] M. Bastero-Gil, S. Bhattacharya, K. Dutta, and M. R. Gangopadhyay, JCAP **02**, 054 (2018), arXiv:1710.10008 [astro-ph.CO].
[105] M. Correa, M. R. Gangopadhyay, N. Jaman, and G. J. Mathews, Phys. Lett. B **835**, 137510 (2022), arXiv:2207.10394 [gr-qc].
[106] M. Correa, M. R. Gangopadhyay, N. Jaman, and G. J. Mathews, Phys. Rev. D **109**, 063539 (2024), arXiv:2306.09641 [astro-ph.CO].